Supplementary Material to Vorlova, Koch et al. “Coagulation factor XII induces pro-inflammatory cytokine responses in macrophages and promotes atherosclerosis in mice”

(Thromb Haemost 2017; 117.1)

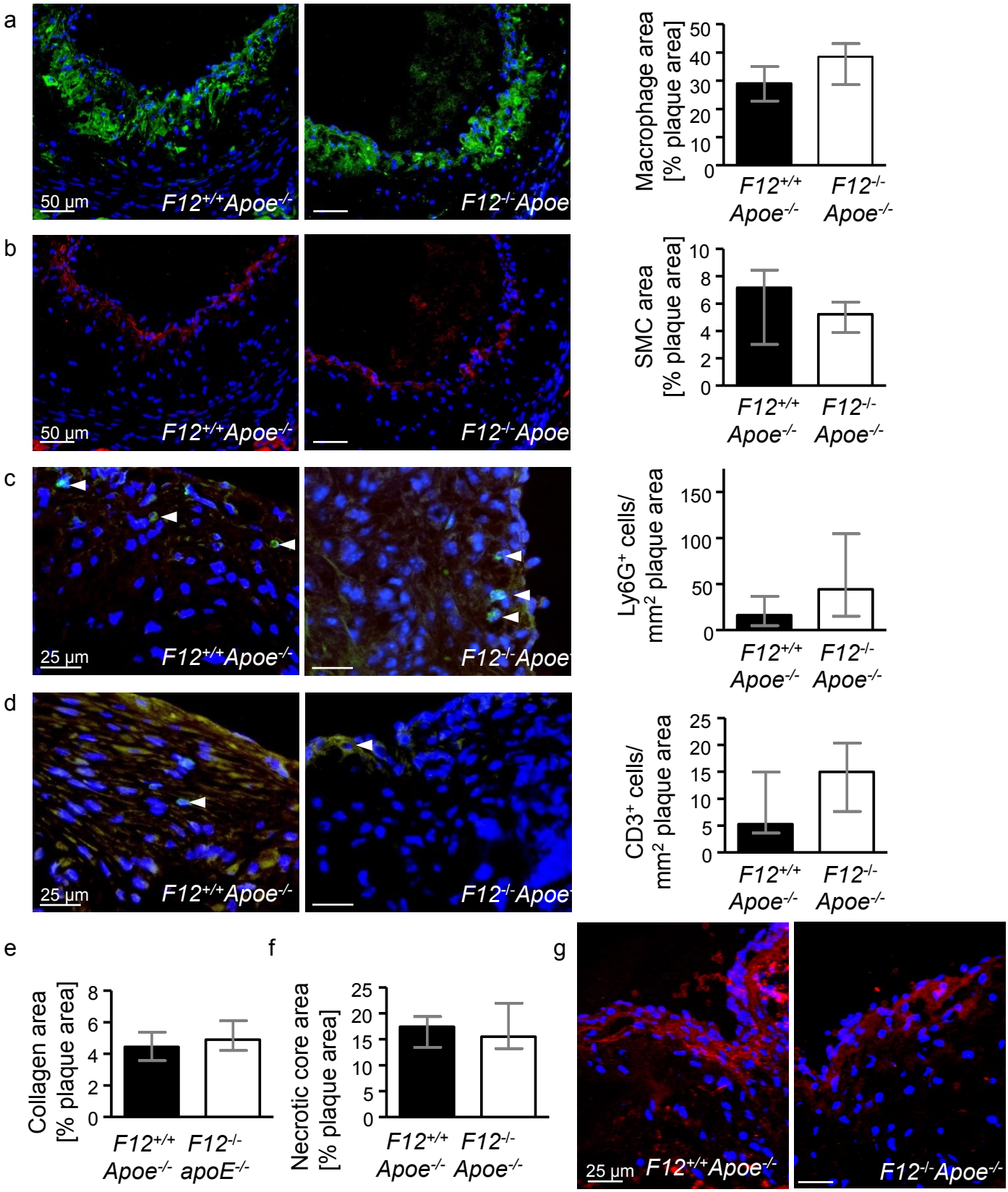

Suppl. Figure 1: Deficiency of FXII in *Apoe*$^{-/-}$ mice does not alter atherosclerotic plaque phenotype. Atherosclerotic lesions were analyzed in *F12*$^{+/+}$*apoE*$^{-/-}$ (n=13 mice) and *F12*$^{-/-}$*apoE*$^{-/-}$ (n=14 mice) mice fed a high fat diet for 12 weeks. (a) Quantification of the Mac-2^{+} (green) macrophage area, (b) α-smooth muscle actin^{+} (red) smooth muscle cell area, (c) Ly6G^{+} (green) neutrophil numbers, (d) CD3^{+} (green) T cell numbers, (d) Sirius-red^{+} collagen area, (e) acellular necrotic core area, and (g) MMP9 (red) staining in aortic root sections. Representative images are shown; nuclei are counterstained with DAPI (blue). Bars represent median with interquartile ranges.

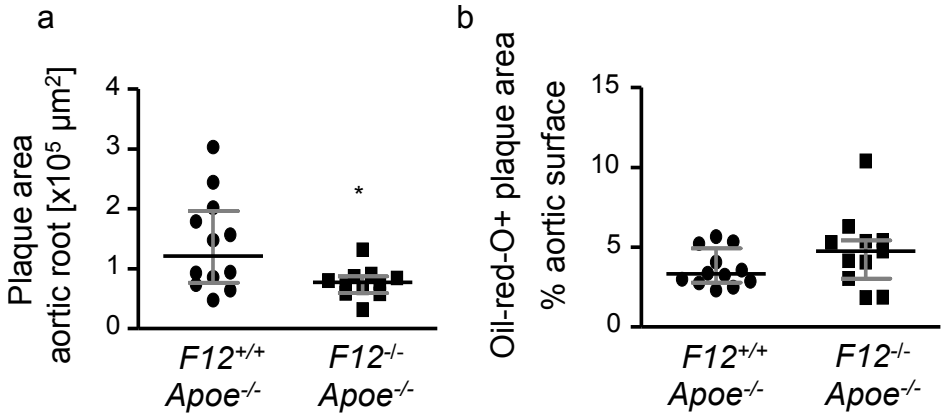

Suppl. Figure 2: Deficiency of FXII in *Apoe*$^{-/-}$ mice reduces atherosclerotic lesion formation in the aortic root but not aorta after 6 weeks of HFD. Atherosclerotic lesion formation was analyzed in *F12*$^{+/+}$*Apoe*$^{-/-}$ (n=12) and *F12*$^{-/-}$*Apoe*$^{-/-}$ (n=11) mice fed a high fat diet for 6 weeks. (a) Quantification of plaque area in Aldehyde-Fuchsin stained aortic root sections and (b) in Oil-Red-O stained aortae. Data represent median with interquartile ranges.

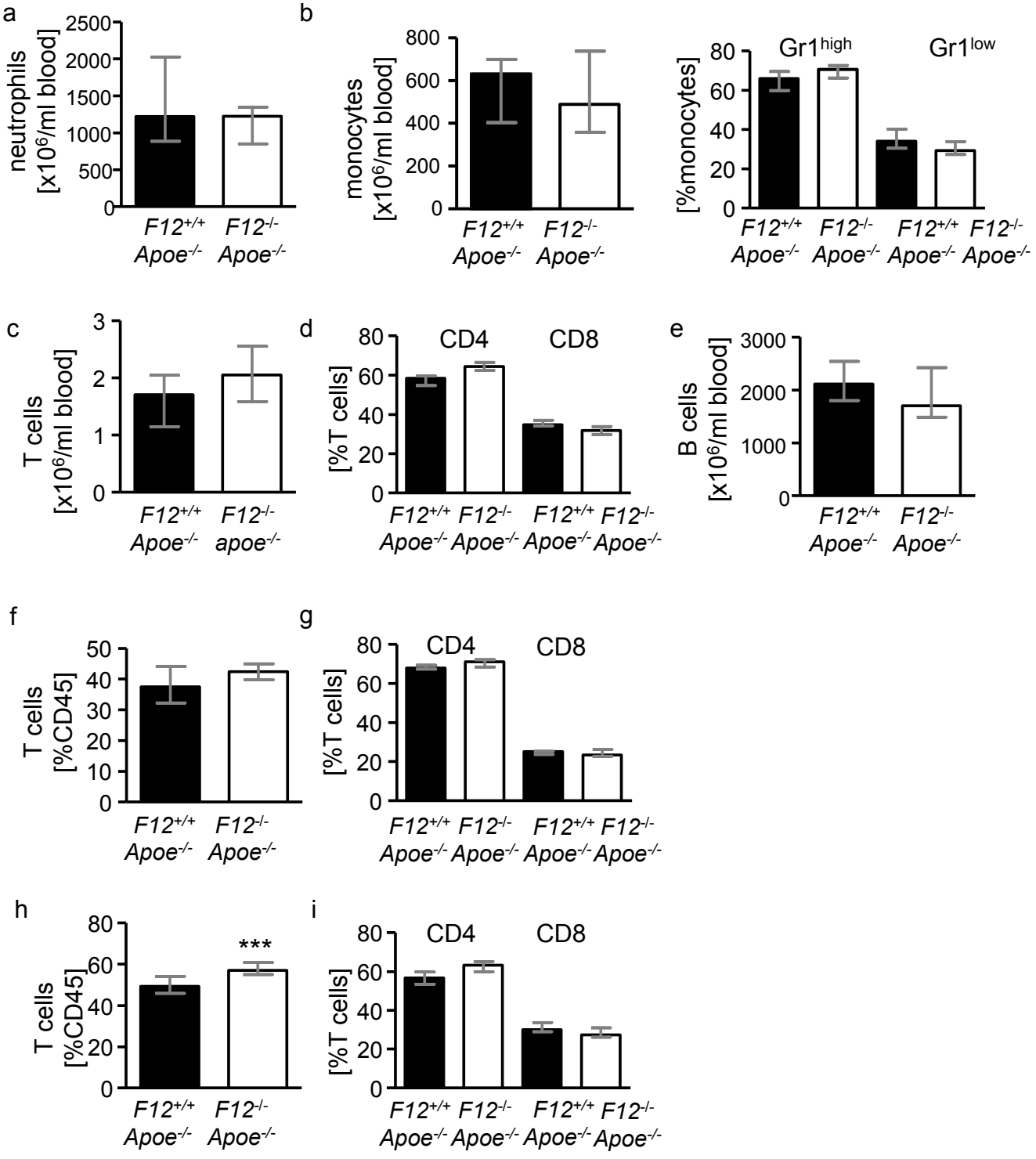

Suppl. Figure 3: Leukocyte distributions in *F12$^{+/+}$Apoe$^{-/-}$ and F12$^{-/-}$Apoe$^{-/-}$ mice.* Flow cytometric analyses of neutrophil (a), monocyte and monocyte subsets (b), T cells (c) and CD4$^+$ and CD8$^+$ T cell distributions, and B cells (d) in blood, and T cell distributions in spleen (f,g) and lymph nodes (h,i) of atherosclerotic *F12$^{+/+}$Apoe$^{-/-}$* (n=10) and *F12$^{-/-}$Apoe$^{-/-}$* mice (n=6) fed a high fat diet for 12 weeks. Bars represent median with interquartile ranges. **p<0.01, ***p<0.001.

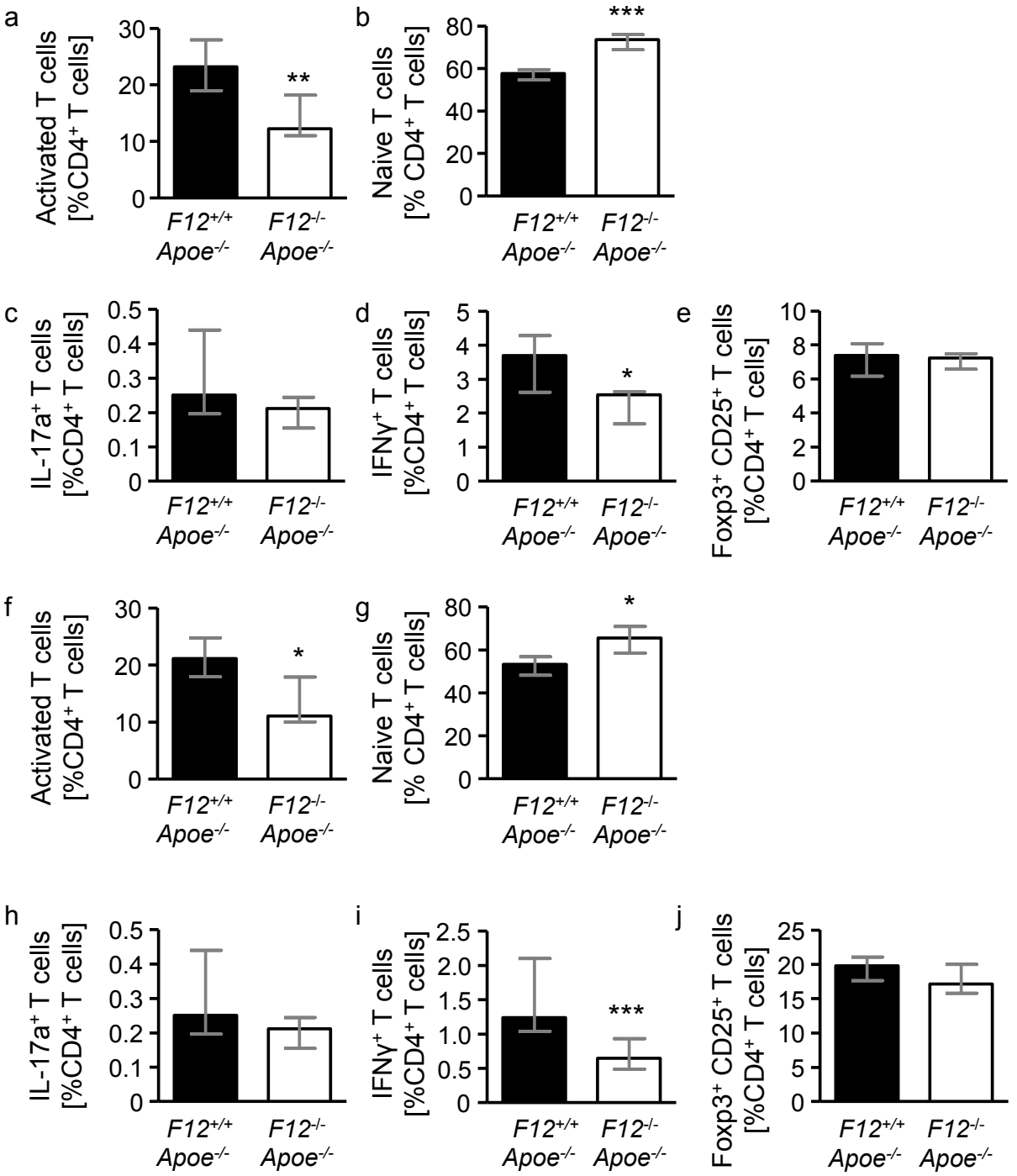

Suppl. Figure 4: *Apoe*$^{-/-}$ mice deficient in FXII display diminished T cell activation. Flow cytometric analyses of activated T cell distributions in blood (a-e) and lymph nodes (f-j) of atherosclerotic *F12*$^{+/+}$*Apoe*$^{-/-}$ (n=10) and *F12*$^{-/-}$*Apoe*$^{-/-}$ mice (n=6) fed a high fat diet for 12 weeks. Frequencies of, activated CD44^{high} CD62L^{low} (a,f) and naïve CD62L^{high} CD44^{low} CD4^{+} T cells (b,g), IL-17a^{+} CD4^{+} T cells (c,h), IFNγ^{+} CD4^{+} T cells (d,i), and of Foxp3^{+}CD25^{+} CD4^{+} T cells (e,j) were quantitated. Bars represent median with interquartile ranges. *p<0.05, **p<0.01, ***p<0.001.

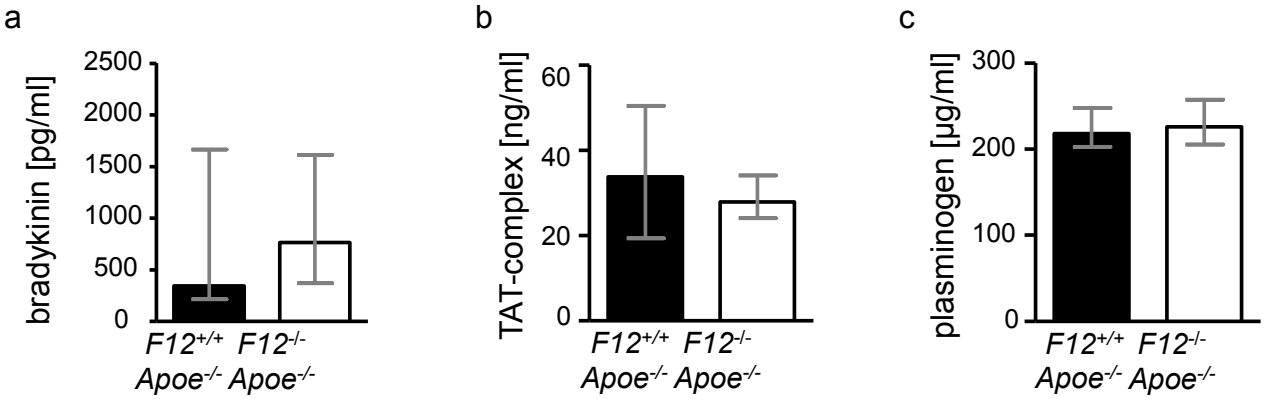

Suppl. Figure 5: Deficiency of FXII in atherosclerotic *Apoe*$^{-/-}$ mice does not alter blood plasminogen, bradykinin, or TAT-complex levels. Bradykinin (a), TAT-complex (b) and plasminogen (c) protein levels in serum or plasma of *F12*$^{+/+}$*Apoe*$^{-/-}$ and *F12*$^{-/-}$*Apoe*$^{-/-}$ mice after 12 weeks of high fat diet feeding, as quantified by ELISA (n=9-16 mice per group). Bars represent median with interquartile ranges.

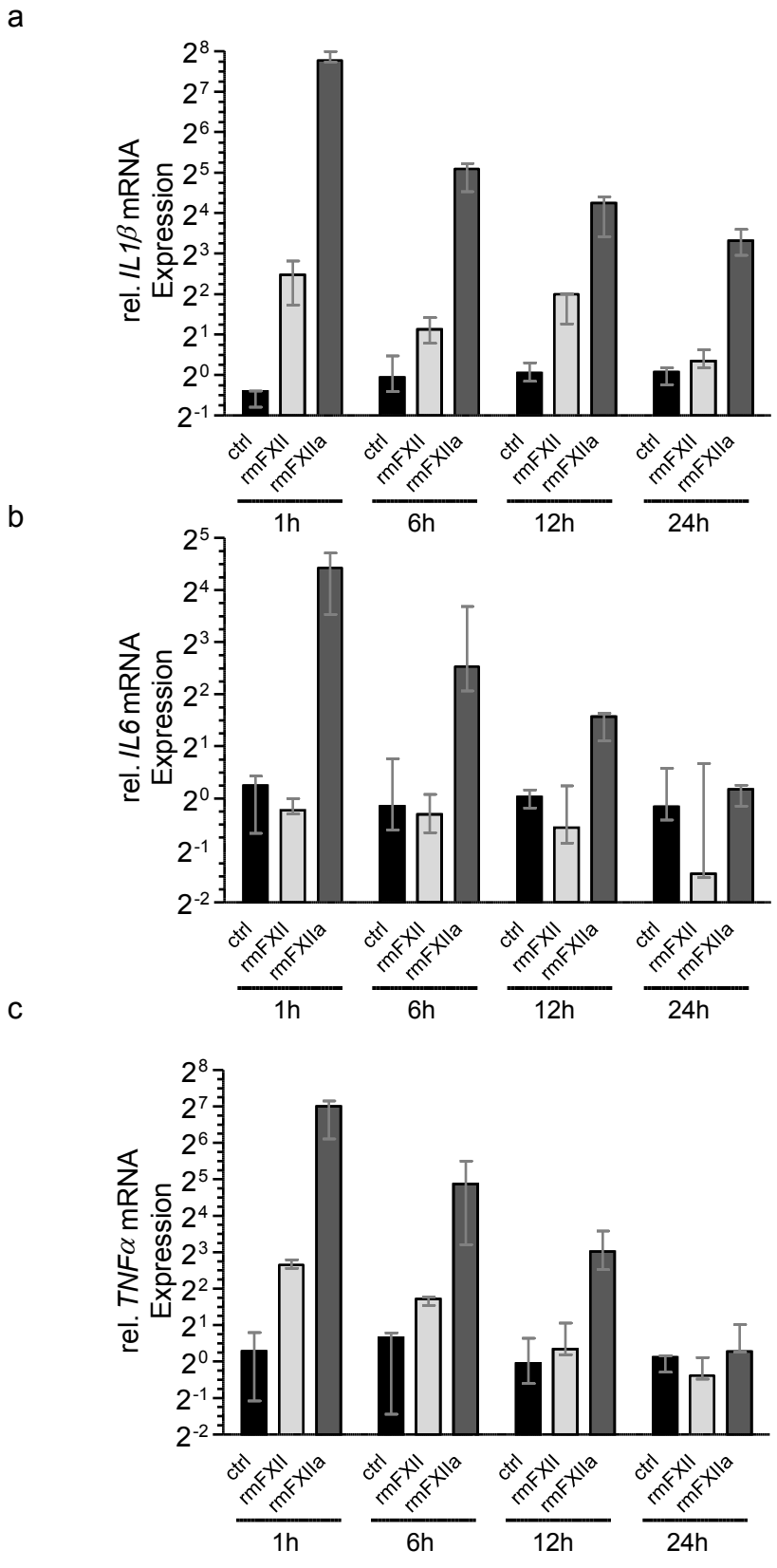

Suppl. Figure 6: Time-dependent induction of cytokine mRNA expression after FXII or FXIIa stimulation in bone marrow-derived macrophages (BMDMs). Cytokine mRNA expression was quantified by real-time PCR at 1, 6, 12 and 24h after 3µg/ml rmFXII or mFXIIa stimulation of BMDMs (n=3 mice). Data represent mean ± SEM.

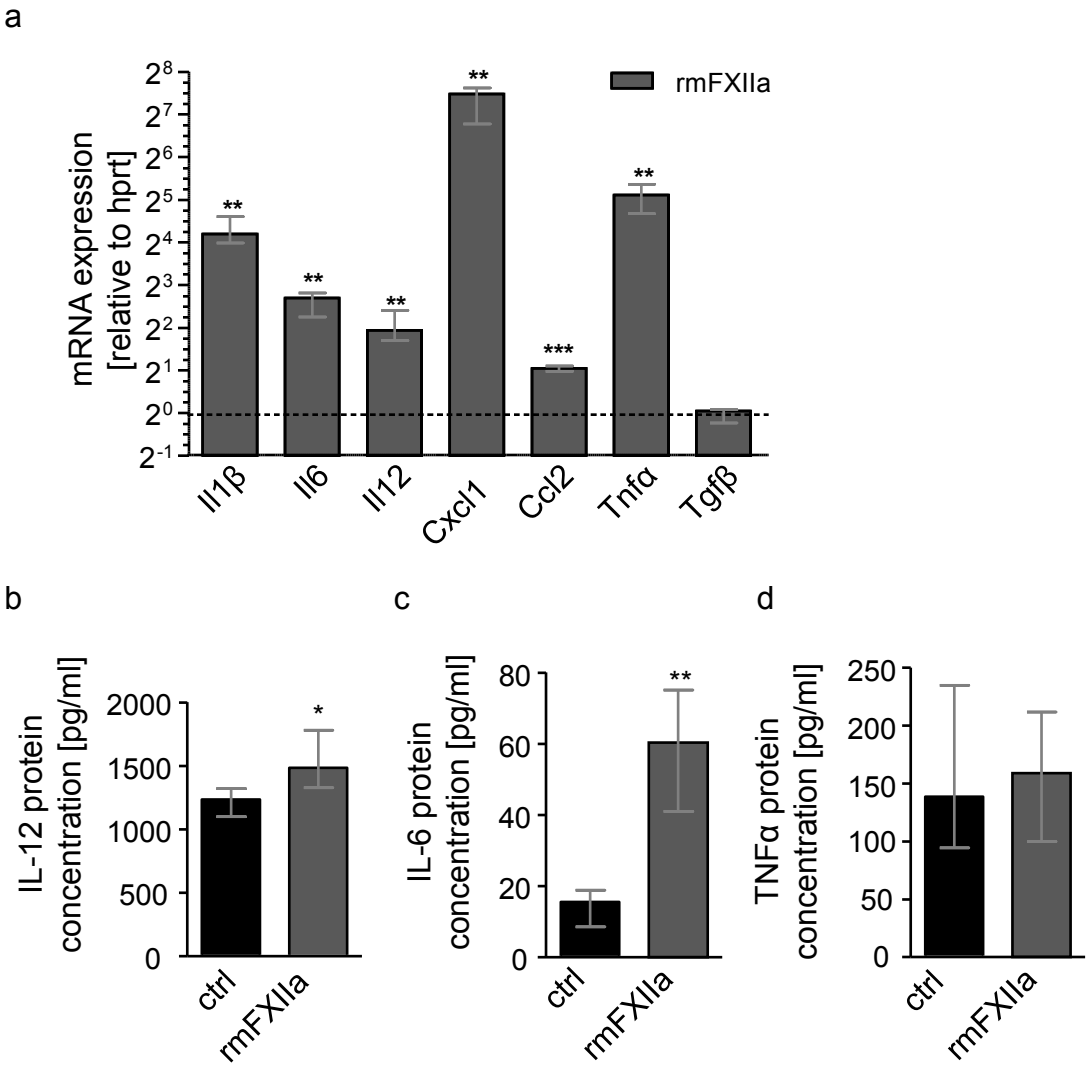

Suppl. Figure 7: Stimulation of bone marrow-derived antigen presenting cells (BM-APCs) with rmFXIIa induces cytokine expression. (a) Induction of cytokine mRNA expression was quantified in BM-APCs after 1h of stimulation with rmFXIIs (n=3 mice) by real time PCR. Protein secretion of (b) IL-12, (c) IL-6 and (d) TNFα into M-APC culture supernatants was quantified after treatment with FXII for 24h by ELISA (n=3). Bars represent median with interquartile ranges. *p<0.05, **p<0.01, ***p<0.001.

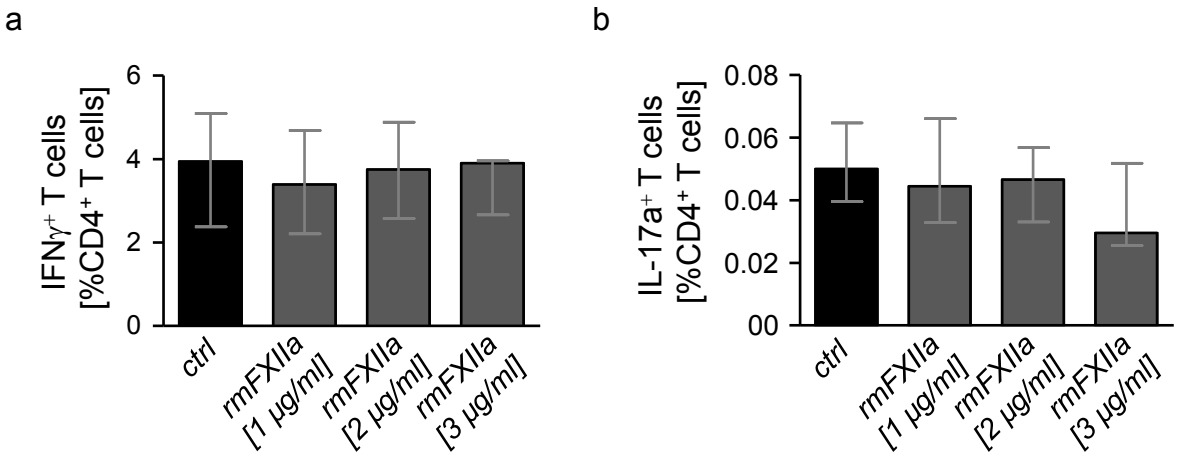

Suppl. Figure 8: Activated FXII does not directly alter T cell polarization. Anti-CD3/CD28 Ab activated naïve CD4+ T cells from C57BL/6J mice stimulated for 3.5 days in the presence or absence of rmFXIIa at indicated concentrations; quantification of (a) IFNγ+ T cells and (b) IL-17a+ T cells (n=4 independent experiments performed in triplicates. Bars represent median with interquartile ranges.

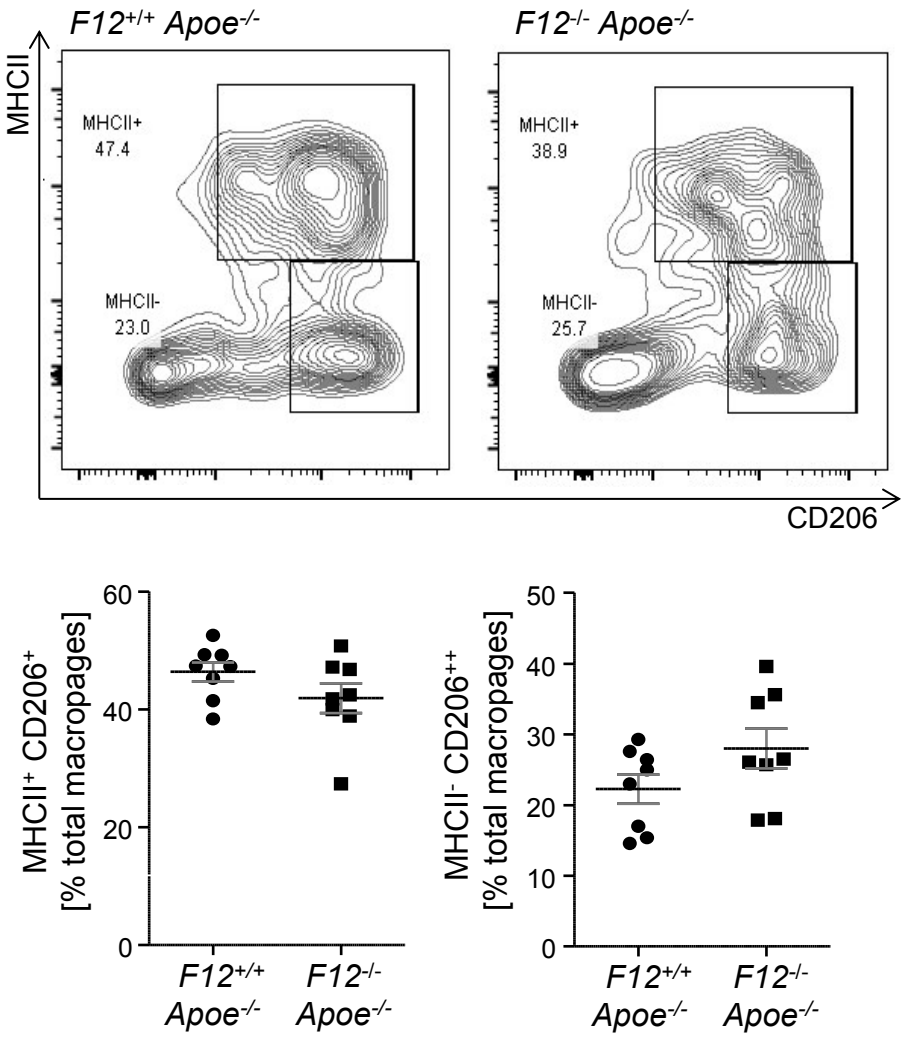

Suppl. Figure 9:. Analysis of lesional macrophage phenotype. Flow cytometric analyses of frequencies of MHCII^{+} CD206^{+} M1 and MHCII^{-} CD206^{++} M2 macrophages among CD11b^{+} F4/80^{+} macrophages in the aorta of atherosclerotic *F12$^{+/+}$Apoe$^{-/-}$* and *F12$^{-/-}$Apoe$^{-/-}$* mice fed a high fat diet for 12 weeks. Representative contour plots are shown. Bars represent median with interquartile ranges.

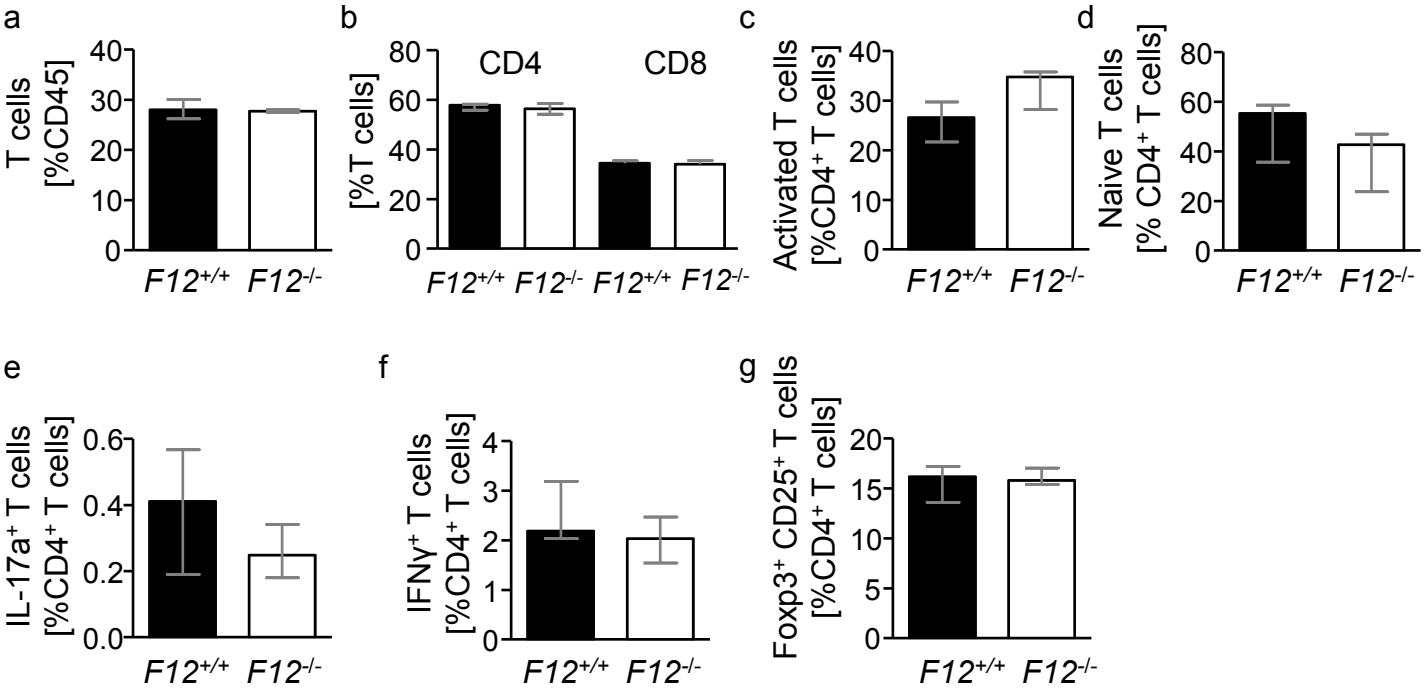

Suppl. Figure 10: Deficiency of FXII does not alter T cell activation under homeostatic conditions. Flow cytometric analyses of T cell distributions in spleens of $F12^{+/+}$ and $F12^{-/-}$ mice (n=5 each). Frequencies of $CD3^+$ T cells among $CD45^+$ cells (a), $CD4^+$ and $CD8^+$ T cells among $CD3^+$ T cells (b), memory effector $CD44^{high}$ $CD62L^{low}$ (c) and naïve $CD62L^{high}$ $CD44^{low}$ $CD4^+$ T cells (d), $IFN\gamma^+$ and IL-$17a^+$ $CD4^+$ T cells (e, f) and of $Foxp3^+CD25^+$ $CD4^+$ T cells (g). Bars represent median with interquartile ranges.

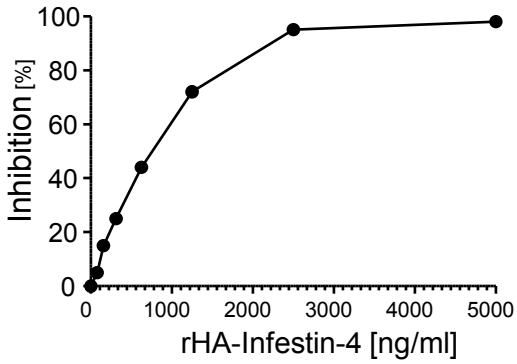

Suppl. Figure 11: Inhibition of FXIIa proteolytic activity. Inhibition of rmFXIIa activity by rHA-Infestin-4 was determined at different inhibitor concentrations and quantified by conversion of a chromogenic substrate for FXIIa.